



Since January 2020 Elsevier has created a COVID-19 resource centre with free information in English and Mandarin on the novel coronavirus COVID-19. The COVID-19 resource centre is hosted on Elsevier Connect, the company's public news and information website.

Elsevier hereby grants permission to make all its COVID-19-related research that is available on the COVID-19 resource centre - including this research content - immediately available in PubMed Central and other publicly funded repositories, such as the WHO COVID database with rights for unrestricted research re-use and analyses in any form or by any means with acknowledgement of the original source. These permissions are granted for free by Elsevier for as long as the COVID-19 resource centre remains active.



A laboratory study of the expiratory airflow and particle dispersion in the stratified indoor environment

Fan Liu^{a,b,c}, Hua Qian^{a,b,*}, Zhiwen Luo^c, Shengqi Wang^{a,b}, Xiaohong Zheng^{a,d}

^a School of Energy and Environment, Southeast University, Nanjing, China

^b Engineering Research Center of BEEE, Ministry of Education, China

^c School of the Built Environment, University of Reading, Reading, United Kingdom

^d Jiangsu Provincial Key Laboratory of Solar Energy Science and Technology, School of Energy and Environment, Southeast University, Nanjing, China

ARTICLE INFO

Keywords:

Expiratory flows

Water tank

Thermal stratification

Lock-up

Particle transport

ABSTRACT

Understanding the role of human expiratory flows on respiratory infection in ventilated environments is useful for taking appropriate interventions to minimize the infection risk. Some studies have predicted the lock-up phenomenon of exhaled flows in stratified environments; however, there is a lack of high-quality experimental data to validate the theoretical models. In addition, how thermal stratification affects the transport of exhaled particles has not been explored so far. In this study, a water tank experiment was conducted according to the similarity protocols to mimic how the expiratory airflow and particles behaved in both uniform and stratified environments. The lock-up phenomenon was visualized and compared with the predicted results by an integral model. Results showed that our previously developed theoretical model of a respiratory airflow was effective to predict the airflow dispersion in stratified environments. Stratification frequency (N) of the background fluid and the Froude Number Fr_0 of the thermal flow jointly determined the lock-up layer in a power law. For the particle dispersion, it indicated that small particles such as fine droplets and droplet nuclei would be 'locked' by indoor thermal stratification, and disperse with the thermal flow over a long distance, potentially increasing the long-range airborne infection risk. Large particles such as large droplets can deposit within a short distance, hardly affected by thermal stratification, however, droplet infection could happen to the susceptible people at a close contact with the infector. This study could give some guidance in view of cross-infection control indoors for stratified environment.

1. Introduction

The possible serious threat of respiratory disease infection in buildings to human health is reiterated by the recently worldwide COVID-19 pandemic [1,2], MERS epidemic in 2013 and 2015 [3], and SARS epidemic in 2003 [4]. Airborne transmission has been recognized as an important transmission route for a number of infectious diseases [5,6], and becomes an important research topic within the indoor air community [7–9]. Many studies show that the airborne routes are directly related to the indoor airflow [10–12]. Inappropriate airflow pattern will cause an accumulation of the exhaled contaminants indoors, especially when a vertical temperature gradient exists [13–15], which largely increases the risk of airborne cross-infection in indoor spaces [16,17]. It is of great significance to analyze the spatial distribution characteristics of the exhaled flow and contaminants in such stratified indoor

environments, as a result, the risk of airborne cross-infection can be controlled and minimized via reasonable precautions.

The studies reporting the indoor thermal stratification could increase the risk of cross-infection are based on two significant findings. First, the exhaled air could travel a longer distance in indoor environment with a vertical temperature gradient, such as in displacement ventilation (DV) [18–21]. Second, the exhaled contaminants could be more easily trapped at a certain height by the thermal stratification, which was referred to the lock-up phenomenon, and therefore higher concentration [13,14,16]. Both findings imply a higher exposure for susceptible people in a thermally-stratified indoor environment. In the work of Bjørn and Nielsen [22], it was found that if the vertical temperature gradient was larger than about 0.4–0.5 °C/m in the real-world case, the lock-up layer can settle in people's breathing zone. Mui et al. [23] reported that the interpersonal exposure to the sneezed contaminants in a stratified

* Corresponding author. School of Energy and Environment, Southeast University, No.2 Sipailou, Nanjing, 210096, China.

E-mail addresses: qianh@seu.edu.cn, keenwa@gmail.com (H. Qian).

<https://doi.org/10.1016/j.buildenv.2020.106988>

Received 17 March 2020; Received in revised form 4 May 2020; Accepted 18 May 2020

Available online 11 June 2020

0360-1323/© 2020 Elsevier Ltd. All rights reserved.

environment was about 2.5 times of that in uniform environment for the face-to-face scenario. Nielsen et al. [13] showed that the exposure in stratified environment increased up to 12 times compared with that in a fully mixed situation for face-to-face cases when the distance between manikins was 35 cm. The exposure risk could reach up to 2 times when distance between manikins becomes 80 cm. All these studies prove that the transmission of exhaled contaminants from one person to another in a thermally-stratified indoor environment could take place directly and increase the danger of cross-infection risk.

There have been abundant studies on the exhaled jet flow dynamics with full-scale experiments in chambers [13,16,18,21,22,24–26], numerical simulations [12,19,22–24,27–29] and analytical models [10,11,15,17,30,31]. These studies revealed that the range of the exhaled contaminant spreading is firstly determined by the exhaled jet flow and subsequently by the ambient airflow. For instance, Qian et al. [16] found that the exhaled droplet nuclei (residues of dried droplets) from a bed-lying manikin were generally well mixed in a room with mix ventilation (MV) whereas a high concentration layer existed in the breathing zone within DV. Lai and Wong [25,26] observed the same phenomena, reporting a higher concentration of the exhaled contaminant (particles of $0.05\ \mu\text{m}$) in the breathing zone in DV than that in MV. Among these experimental studies, the exhaled air distribution and contaminant concentration were mainly measured by using either smoke visualization or tracer gas. However, tracer gas is little influenced by gravity compared to buoyancy, and the experimental works are therefore only valid for the situation when droplets or droplet nuclei are smaller than $5\text{--}10\ \mu\text{m}$ that can follow the persons' exhalation flows and the ambient airflows [13]. In fact, the diameters of the exhaled droplets range from $1\ \mu\text{m}$ to $2000\ \mu\text{m}$ [32]. The transport behaviors of large droplets are different from those of small droplets and gaseous contaminants due to the relatively large gravity and drag force. The dispersion of respiratory droplets was extensively explored in numerical simulation based on the CFD method. As proposed by Redrow et al. [30] and Liu et al. [12], the travelling distance of the exhaled droplets was related to the initial size, relative humidity, breathing mode and ventilation. It was until recently that Ji et al. [27] compared the evaporation and dispersion of exhaled droplets in MV and DV, and found that a non-uniform environment had an obvious impact on the droplet movement. However, the mechanism of thermal stratification on this phenomenon was not explored further. In addition, the numerical results are significantly influenced by the grid resolutions, turbulence closure and initial and boundary conditions. The results must be validated by comparing with laboratory or full-scale experiments.

The theoretical methods relying on the holistic understanding of the interaction of the exhaled jet flow and droplet dynamics are of paramount significance. The trajectories of exhaled airflow and the travel characteristics of large droplets can be calculated and discussed by using empirical formulas, as stated in the work of Xie [10], Wei and Li [11], and Liu et al. [31]. Most of the existing theoretical models can be only applied into the ideal conditions with the absence of room airflow and temperature variation. However, a real exhalation exhibits a more complex interaction between the ambient air and exhaled air. Later on, Zhou et al. [15] put forward a non-dimensional theoretical buoyant jet model to obtain the centerline of the jet in thermally-stratified indoor environments. Based on his work, a jet integral model in a thermally stratified environment is proposed in our previous study [17]. The model can be used in different ventilated rooms (i.e., MV, DV and personalized ventilation), with various human-to-human orientations, to predict the personal exposure and obtain a relatively safe range for susceptible persons. However, the model was only validated by very limited experimental observations in the literature. More comprehensive experimental scenarios are needed to test the validity of our model.

Overall, there is still a lack of understanding of combined effect of indoor thermal stratification and exhaled contaminants, and two issues in existing studies have been not elaborated in details, i.e., how to accurately validate the existing theoretical models of an expiratory jet

flow under a controllable thermal environment, and how to characterize the distribution of the exhaled droplets with different sizes in a stratified environment (as shown in Fig. 1). As reviewed above, full-scale experiments in ventilated chambers are often limited to several airflow patterns, in which it is difficult to control vertical temperature gradient as needed. Those experiment data were pretty good for specified airflow pattern or airflow rate in a specified space (especially for height). However, those experiment data might not be easy to use for general purposes. Logistical difficulties of experiments in air surrounding have promoted a number of fluid modeling following similarity protocols. Water-tank modeling has been proved to be an appropriate tool to simulate the air environment with different ventilation types. For example, Hunt and Linden [33] studied natural ventilation by the combined effects of buoyancy and wind for a small-scale room or building in a water tank. Davies Wykes [34] also used a reduced-scale model room in a water tank to examine the effect of indoor-outdoor temperature difference on the transient wind-driven cross-ventilation. Apart from the indoor environment, water tank is greatly used for the dispersion of atmospheric pollutants under calm and stably stratified conditions, especially in urban heat island circulation (UHC) [35,36]. Besides of time and expense reducing, water tank modelling is easy to control boundary conditions and to observe. Two-tank method based on the Modified Oster method [37] is the most common method to produce a stable density stratification in water. The tank is slowly filled through tubes on the bottom with thin layers of salt water, each layer increasing in specific gravity [38]. The limitation of two-tank method is that the created stratified layer cannot be recycled and reused, causing a large amount of water waste. Another method for producing stratification in water is by heating and cooling, i.e., heating at the top and cooling at the bottom [39–42]. It has been well recognized that experimental parameters in these water-tank models can be individually controlled to resolve the effects of each variable. Moreover, conductivity meters for salt and thermistors or thermochromic liquid crystals (TCL) for temperature can be quite fast-response devices in water. They offer possibilities for the measurement or visualization of the concentration and temperature distribution [35,36]. However, studies have been rarely carried out to understand the real-human exhalation behaviors in the water fluid. In the work of Wei and Li [43], a protocol for scaling particle experiments between air and water was proposed, but only suitable for the isothermal jet in a thermally uniform environment. Further experimental studies on the lock-up phenomenon of the exhaled jet flow and the transport of the exhaled particles in a thermally stratified environment are necessary.

In this study, the water tank with well controllable settings (temperature gradients) and quite fast-response devices for temperature distribution or particle tracking are used to fill the above research gaps

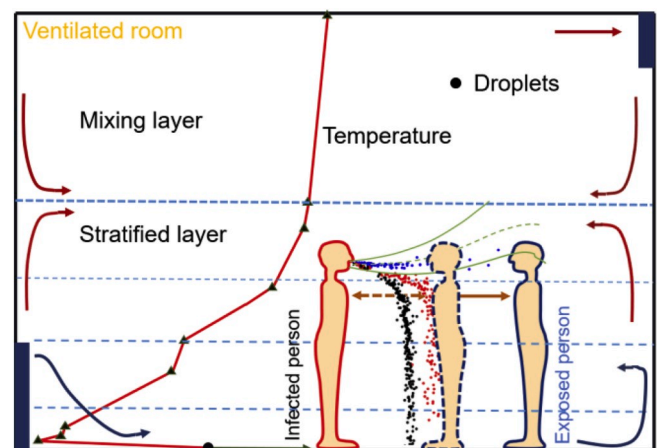


Fig. 1. Illustration of the respiratory airflow and exhaled droplets in a thermally-stratified indoor environment.

which are easy to observe. Two critical purposes of this study are: Scaling the expiratory airflow and particles under feasible and controllable water-tank settings to explore the impact of thermal stratification on the transport of exhaled particles which may occurred widely in different airflow patterns and large space, and obtaining high-quality experimental data to validate the potential models based on the simplified assumptions. It is also expected to give some guidance in view of cross-infection control of respiratory diseases in ventilated built environments.

2. Similarity analysis and modeling criteria

To simplify the complex breathing modes, the respiratory airflow exhaled from the mouth or nostril are considered as a non-isothermal buoyant jet, evolving in indoor air environments [15,17]. The constant velocity is used to represent the pulsating breathing mode, which may cause a little higher estimation of airflow and particle dispersion, but meet the actual needs of the evaluation of cross-infection risk for emergency response. For a viscous, incompressible and stratified fluid, the governing equations of motion and thermodynamic energy are analogous in air and water systems. However, similarity requirements should be satisfied to mimic the flow dynamics of an expiratory jet flow using a reduced-scale model in the tank. In this experiment, the water tank is used to simulate an indoor environment with or without thermal stratification. The human mouth will be scaled into a circular orifice, with the jet flow being discharged from a L-like nozzle. The discharged flow will firstly be heated to create an initial temperature difference with the ambient fluid in the water tank, and gradually evolve within the water.

2.1. Similarity requirements of the exhalation jet flow

Non-dimensional forms of the governing equations of motion and thermodynamic energy in a stratified fluid are similar to those in Lu et al. [42]. For a thermal jet flow, the dynamic similarity between laboratory experiments and real situations can be achieved by the Reynolds number Re . A typical value of Re for an expiratory behavior ranges from 2,500 to 12,500, with mouth diameter of 2 cm, and breathing velocities of 2–10 m/s [10]. The Re attainable in the reduced-scale water tank model is about 2,000 to 8,000, with the opening size of 4 mm and initial velocities of 0.5–2 m/s (see Table 1), a little small for a rigorous simulation. However, both the Re values in air and water systems keep above the critical value ($Re = 2,000$) that is required for fully turbulent flow, in which cases the mean flow and large eddy structure could be modeled correctly regardless of the differences in microscale eddies which have little dispersive effects. That means, the jet flow becomes independent of Re [44]. Therefore, for the turbulent jet flow in a stratified fluid, the Froude number Fr becomes the governing criterion for describing the prototype flow, which must be duplicated in the laboratory model

$$Fr = \frac{u_c}{\sqrt{g_c D}} \quad (1)$$

where u_c is the axial velocity of jet flow (m/s), $g_c = (\rho_a(z) - \rho_c)g/\rho_{ref}$ is the buoyant acceleration (m/s²), ρ_c the axial density of jet flow (kg/m³), $\rho_a(z)$ the ambient air density (kg/m³) and ρ_{ref} a constant reference density (kg/m³) with the Boussinesq approximation [17].

It should be noted from Eq. (1) that when considering water as the ambient fluid for modeling in the experiment, it is necessary to define Fr in terms of density, rather than temperature. The protocol for scaling buoyant jet flow experiments between air and water in thermally uniform and stratified environments is discussed below.

In a thermally uniform environment, according to Eq. (1) the initial conditions in two uniform systems need to satisfy

$$\frac{u_{c,g}}{\sqrt{g D_g (\Delta\rho_c/\rho_{ref})_g}} = \frac{u_{c,w}}{\sqrt{g D_w (\Delta\rho_c/\rho_{ref})_w}} \quad (2)$$

$$\frac{u_{c,g}}{u_{c,w}} = \sqrt{\frac{D_g (\Delta\rho_c/\rho_{ref})_g}{D_w (\Delta\rho_c/\rho_{ref})_w}} \quad (3)$$

where the subscript g stands for air (distinguished from the subscript a for indoor ambient air), and w for water.

The ambient air temperature at the exhalation outlet is 20 °C, and 34 °C for the exhaled air [45]. The mouth diameter is 2 cm [17], and exhalation velocity ranges from 2 m/s (breathing) to 10 m/s (coughing). The ambient water temperature in the tank is close to 20 °C. Both the diameter of L-like nozzle model and the initial temperature of thermal jet are basic controlling variables in the water-tank experiment. Therefore, the initial velocity of the thermal jet, i.e., the water pressure difference is determined in the experiment.

In a stratified environment, Fr is defined as

$$Fr = \frac{u_c}{DN} \quad (4)$$

In which, the buoyancy frequency $N = \sqrt{-\frac{g}{\rho_{ref}} \frac{d\rho_a}{dz}}$ is the angular frequency at which a vertically displaced parcel will oscillate within a stratified stable environment. Here it is used to denote the initial thermal stratification intensity of water in the tank. The boundary conditions in two stratified systems need to satisfy

$$\frac{u_{c,g}}{D_g \sqrt{g/\rho_{ref,g} (d\rho_a/dz)_g}} = \frac{u_{c,w}}{D_w \sqrt{g/\rho_{ref,w} (d\rho_a/dz)_w}} \quad (5)$$

$$\frac{(d\rho_a/dz)_g}{(d\rho_a/dz)_w} = \frac{\rho_{ref,g}}{\rho_{ref,w}} \frac{u_{c,g}^2}{u_{c,w}^2} \frac{D_w^2}{D_g^2} \quad (6)$$

Table 1

Experimental parameters for a total of 9 cases, which are grouped into 3 scenarios.

Scenario	Case	In air					In water						
		$dT_0/dz(^{\circ}\text{C}/\text{m})$	$T_c(^{\circ}\text{C})$	$D(\text{m})$	$u_D(\text{m/s})$	$N_{\text{air}}(\text{s}^{-1})$	$T_c(^{\circ}\text{C})$	$D(\text{m})$	$u_D(\text{m/s})$	$\Delta H(\text{cm})$	$dT_0/dz(^{\circ}\text{C}/\text{cm})$	$N_{\text{water}}(\text{s}^{-1})$	Fr
1	1	0	34	0.020	5	–	55	0.004	1.10	6.20	0	–	50
	2	1	34	0.020	5	0.166	55	0.004	1.10	6.20	0.154	0.183	1503
	3	2	34	0.020	5	0.235	55	0.004	1.10	6.20	0.309	0.259	1063
	4	4	34	0.020	5	0.333	55	0.004	1.10	6.20	0.617	0.366	752
	5	6	34	0.020	5	0.407	55	0.004	1.10	6.20	0.926	0.449	614
2	6	2	34	0.020	2	0.235	55	0.004	0.45	1.00	0.309	0.259	425
	3	2	34	0.020	5	0.235	55	0.004	1.10	6.20	0.309	0.259	1063
	7	2	34	0.020	10	0.235	55	0.004	2.20	24.80	0.309	0.259	2126
3	8	2	34	0.150	5	0.235	55	0.003	1.10	6.20	0.309	0.259	1417
	3	2	34	0.020	5	0.235	55	0.004	1.10	6.20	0.309	0.259	1063
	9	2	34	0.025	5	0.235	55	0.005	1.10	6.20	0.309	0.259	851

For the air and water fluid in two systems, the fluid density changes with the temperature, with fitted relationships shown in Fig. 2, so Eq. (6) can be converted into

$$\frac{(d\rho_a/dz)_g}{(d\rho_a/dz)_w} = \frac{0.2217 \rho_{ref,g} u_{c,g}^2 D_w^2}{0.0034 \rho_{ref,w} u_{c,w}^2 D_g^2} \quad (7)$$

Temperature gradient is assumed to range from 1 °C/m to 6 °C/m in a thermally-stratified indoor environment. The initial velocity of the thermal jet in the laboratory model is known from Eq. (3). The temperature gradient of the water can be obtained according to Eq. (7), by which the heating temperature at the top and cooling temperature at the bottom can also be determined in the experiment.

2.2. Similarity requirements of the exhaled particles

In this experiment, the exhaled droplets and droplet nuclei are simulated by glass beads, without considering the evaporation process of droplets in the water-tank experiments. The detailed protocol for scaling particle experiments between air and water is referred to the work of Wei and Li [43]. To make particle motions comparable in two stratified systems, it needs to make the Stokes number duplicated, which is defined as

$$St = \frac{u_c \tau}{D} \quad (8)$$

where τ is the relaxation time, given by

$$\tau = \frac{\rho_p d_p^2}{18\mu} \quad (9)$$

Thus,

$$St_g = St_w \quad (10)$$

i.e.,

$$\frac{d_{p,g}}{d_{p,w}} = \sqrt{\frac{\rho_{p,w} u_{c,w} v_g \rho_g D_g}{\rho_{p,g} u_{c,g} v_w \rho_w D_w}} \quad (11)$$

Glass beads ($\rho = 2,480 \text{ kg/m}^3$) of three size categories are used in the experiments to analogize the particle sizes in realistic human: 43–75 μm (small particles of 10–20 μm), 180–300 μm (medium particles of 50–80 μm) and 425–600 μm (small particles of 110–160 μm).

3. Experimental set-up and case description

Experiments are performed in a transparent glass rectangular tank (Length \times Width \times Height = 2.4 m \times 0.8 m \times 0.8 m) filled with water at rest. The tank walls are made of 1.5-cm-thick glass to be transparent to the green laser sheet. The experimental apparatus includes stable jet

flow system, thermal stratification system and monitoring system, as illustrated in Fig. 3. The L-like nozzle (⑤ in Fig. 3) is placed horizontally at a depth of 25 cm below the water surface. The vertical cross-section is illuminated by a laser sheet or by vertical placement of two thermochromic liquid crystal (TLC) sheets (⑧ in Fig. 3). Stable stratification with a vertical temperature profile of water is created using the heating and cooling method.

①Heated liquid vessel; ②Separator vessel; ③Overflow collector; ④Support; ⑤L-like nozzle; ⑥Ambient liquid; ⑦Thermocouple; ⑧TCL or Laser sheet; ⑨Support; ⑩Camera; ⑪Heating coil; ⑫Cooling coil.

In all experiments, the heated liquid is first injected into Separator vessel (② in Fig. 3) until its level reaches the overflow surface. Then the upper valve is opened, and the heated liquid is then injected into Heated liquid vessel (① in Fig. 3) to ensure a sustaining overflow status of Separator vessel before opening the lower valve. A peristaltic pump (Kamoer Lab UIP WIFI-S183, China) is used here to continuously supply heated liquid for Heated liquid vessel. After these procedures, the lower valve is opened, then the liquid is injected into the ambient fluid with lower temperature in the water tank through the L-like jet nozzle, and a submerged horizontal round thermal jet is formed. The change of the ambient liquid level induced by the discharged thermal jet flow is less than $5 \times 10^{-5} \text{ m}$, making a small change in jet velocity of less than 0.05 m/s. Therefore, it can be considered that the overflow state in the separator vessel keeps the outlet velocity of the L-like nozzle stable during the process. In indoor environments, the ratio of the mouth/nostril diameter (2 cm) and room size (3–5 m) is on the order of about 1:250–1:150. In this study, the corresponding ratio of the orifice size of L-like nozzle (3–5 mm) and water-tank size (0.8–2.4 m) is on the order of about 1:800–1:160, so it can be considered that water tank is large enough for the injected flow to fully develop in water space. In particle transport experiments, glass beads are seeded into the discharged fluid from the top of Separator vessel by using an hourglass to ensure a uniform velocity distribution of the particles at the L-like nozzle exit.

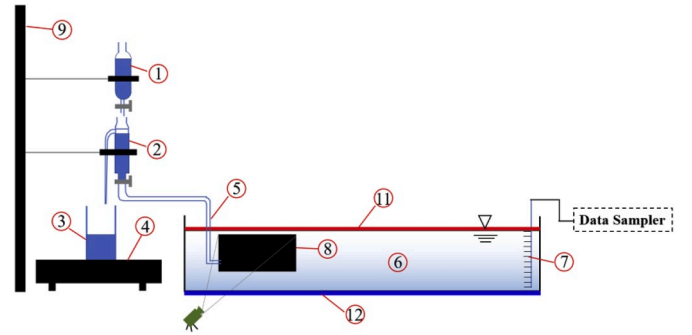
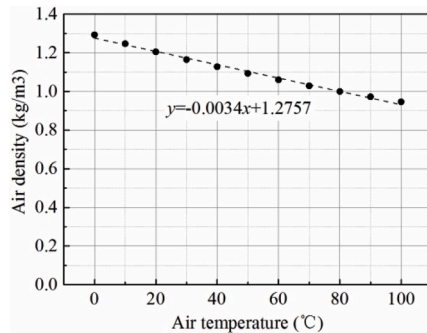
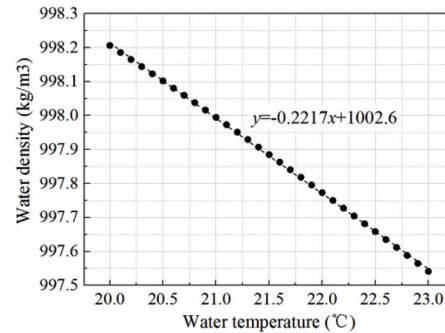


Fig. 3. Sketch of the experimental set-up.



(a)



(b)

Fig. 2. Linear relationships between the density and temperature in two systems: (a) air density; (b) water density.

Particles of three size categories are respectively released in three experiments. The particle volume ratio in the thermal flow is below 0.5% so that the flow is not affected by the adding of particles.

To create a thermally stratified environment, a U-type heating coil (Ⓔ in Fig. 3) and a low-temperature thermostat (DC-1050, China) are used to prepare the stratified water in the tank. The low-temperature thermostat is connected with the cooling coil (Ⓒ in Fig. 3) at the bottom of the water tank by water pipes to form a circulation loop. The experimental rig is shown in Fig. 4(a). Both the water tank and low-temperature thermostat are initially filled with water, and the screws on the heating coil are adjusted to make the U-type heating coil just immersed by water surface. A temperature controller is fixed to measure and control the temperature of the water surface. After turning on the power of the heating coil, a targeted temperature is set and displayed on the temperature controller. Heating starts when the set temperature is higher than the measured temperature; otherwise, heating stops. Similarly, a cooling temperature is set on the low-temperature thermostat and the cooling circulation function is carried out after the thermostat operates normally. The temperature profile measurement of the water is conducted by 16 thermocouples (Ⓓ in Fig. 3), all calibrated and connected to a digital temperature logger (Agilent™ 34970A). The whole process takes 3–4h to make a stable temperature stratification.

The temperature field of thermal jet flow is visualized by two TCL sheets (Edmund Optics Inc., Barrington, NJ, USA; temperature range: 20–25 °C), which are mounted on a support made of acrylic plates so that they can be moved easily into and out of the water, seeing Fig. 4(b). The TCL color changes from blue to red as the temperature varies from

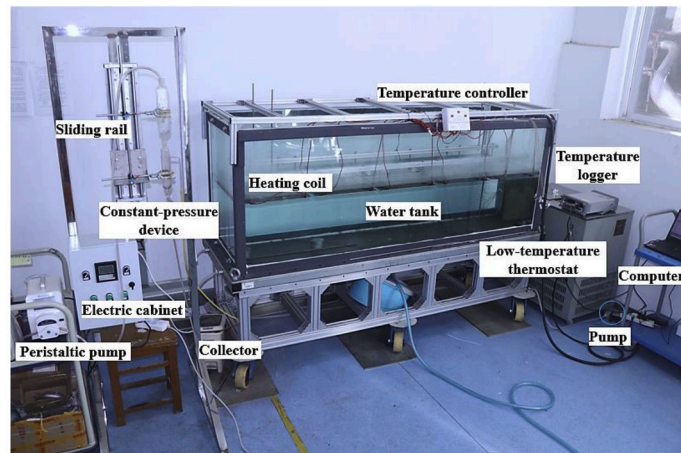
the highest (25 °C) to the lowest (20 °C). To track the lock-up phenomenon of the emitted thermal jet, blue food dye is used to visualize the trajectory. In the particle-release experiments, the mid-sagittal plane of the L-like nozzle is illuminated by a 3-mm laser sheet produced by a 3W DPSS 532 nm laser projector (Ourslux Lighting Technology Co, Ltd) to visualize the distribution of particles, seeing Fig. 4(c). The Canon 77D camera is used to obtain the image of the thermal flow and particle dispersion.

This study aims to investigate the evolution of the exhaled flow in a thermally stratified environment. We consider the impacts of temperature gradients (Scenario 1, Cases 1–5), exhalation velocities (Scenario 2, Cases 6,3,7) and opening sizes (Scenario 3, Cases 8,3,9). All cases are listed in Table 1. The background water in the tank is regarded to be initially uniform, so it can be directly used for Case 1. For Cases 2–9, stable thermal stratification of the water is created using the heating and cooling method described above before each experiment. The created background temperature profiles for the cases using the heating and cooling method are shown in Fig. 5.

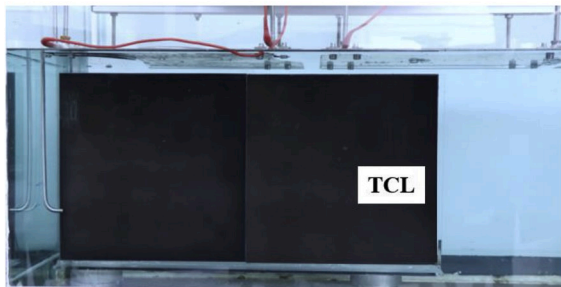
4. Results and discussion

4.1. Temperature attenuation of the thermal flow

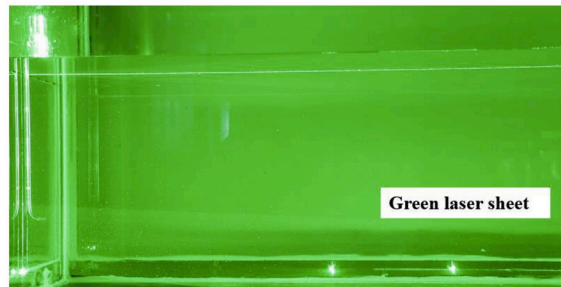
Temperature visualization of the thermal jet flow by TCL sheets and theoretical prediction by jet integral model in thermally uniform environment are shown in Fig. 6. As shown in Fig. 6(a), the background color of the TCL sheets is black. The color turns blue at the initial region of the



(a)



(b)



(c)

Fig. 4. Photos of the experimental rig: (a) The set-up front view; (b) Placement of TCL in the water tank; (c) Green laser sheet through the water. (For interpretation of the references to color in this figure legend, the reader is referred to the Web version of this article.)

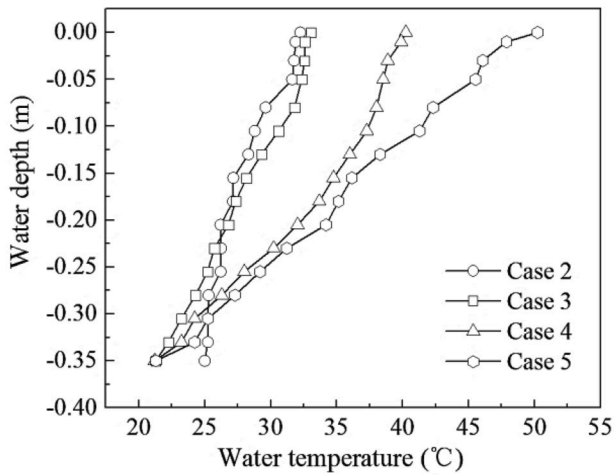


Fig. 5. The vertical temperature profiles of the thermally stratified water in tank.

thermal flow due to its higher temperature, and decays to green along axial and radial distance. At about 40s, the temperature attenuation in the experiment reaches a stable profile. It should be noted that TLC sheets are not being used to map the accurate temperature field but as a qualitative tool to show the trend. The same conditions are repeated in the integral model of thermal flow to obtain the predicted temperature distribution, as shown in Fig. 6 (b). It can be found that in the evolution of the non-isothermal flow, the temperature exhibits an upward attenuation until water surface. In addition, a faster attenuation is observed along the radial distance than the axial distance, which may be induced by the entrainment of the ambient fluid into the jet flow.

The experimental and predicted results of temperature attenuation in a stratified environment are shown in Fig. 7. The background color of

the TCL sheets is stratified due to the temperature gradient of the water. The flow temperature peaks at the initial region, where the color of TCL sheets shows in blue, similar to the observations in the uniform case. At about 40s, the flow temperature cannot further decrease along vertical direction when it equals to the background temperature, as shown in Fig. 7(a). In this case the finally diluted thermal flow will remain submerged, causing no change of the water surface temperature. The corresponding prediction is shown in Fig. 7(b). It can also be found an obvious hump exists in the temperature contour, and the peripheral temperature of the hump is lower than its surrounding.

The physical explanation of the observed phenomenon is illustrated by Fig. 8. Temperature stratification, in nature, is density stratification. For the thermal flow, the rising of the fluid is jointly driven by its momentum and buoyancy. Buoyancy is the results of the density difference between the rising flow ρ_{jet} and the ambient fluid at the height of the jet flow ρ_a . With the dilution, the density difference disappears at a 'stable level' (point A), and the further rise of the flow to the maximum height depends on the jet inertia at this height. The upward displacement of the jet flow will make the fluid heavier than its ambient fluid and hence tends to fall back to its stable position. Conversely, the flow moved downward will become lighter than its ambient fluid and also tends to return to its stable position. This process is repeated, and thus, it results in an oscillation phenomenon at the 'stable level', which refers to the lock-up phenomenon in indoor environments [17]. Fig. 8(b) shows the visualization of the thermal jet flow with blue food dye in the stratified environment (Case 5), as well as the prediction using integral model. The photographic observation clearly shows the flow goes from vertical to horizontal and becomes submerged. In the initial phase the buoyant flow overshoots to a maximum distance of z_m , and then falls back to a distance of z_l and spreading with oscillations at the lock-up height. This behavior is also well predicted in trajectory by the integral model. Comparably, under an outdoor atmospheric condition with a temperature inversion layer, temperature stratification also acts as an effective barrier to further dispersion, making an emitted plume finally to

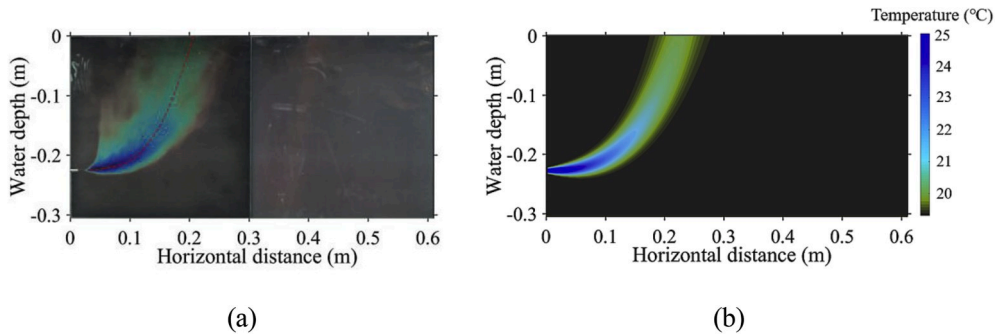


Fig. 6. Temperature attenuation of the thermal flow in uniform environment: (a) experimental temperature visualization (Case 2); (b) calculated temperature distribution.

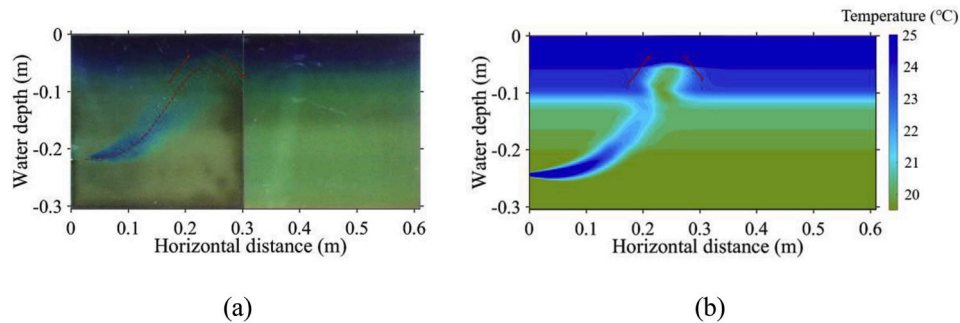


Fig. 7. Comparison of the experimental result with the predicted by integral model of expiratory jet in thermally stratified environment: (a) Experimental temperature visualization (Case 2); (b) Calculated temperature distribution.

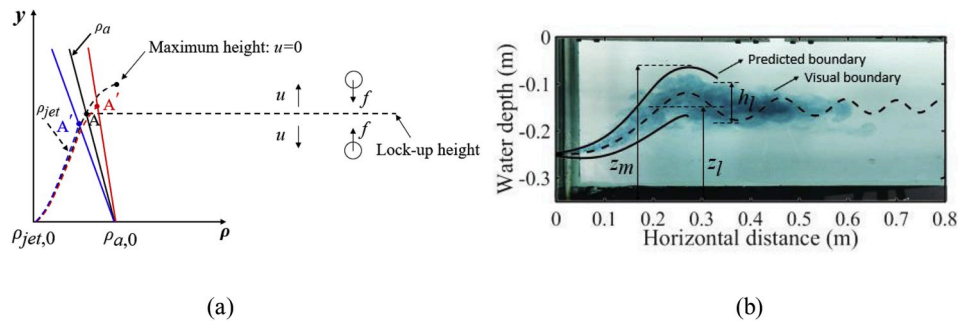


Fig. 8. Illustration of the thermal flow oscillation in a stratified environment: (a) Density variation of a thermal jet flow; (b) Visualization of the thermal jet trajectory in the stratified water-tank of Case 4.

stabilize at a certain height [46]. However, the lock-up phenomenon of a human expiratory flow seems to be different from the plume rising where the momentum contribution is small and usually ignored. In addition, the trajectory with an oscillation of an expiratory jet is a flow trajectory that represents a mass and energy transfer, rather than a single energy transfer.

4.2. The impact of the indoor stratification intensity (scenario 1)

Scenario 1 in Table 1 is designed to explore the dispersion of the thermal jet flow with different temperature gradients. The temperature gradient in indoor environments varies from 1 °C/m to 6 °C/m, which could cover most cases in a stratified room in buildings. The corresponding temperature gradient of the background water in the tank ranges from 0.154 °C/cm to 0.926 °C/cm, with N increasing from 0.183 s^{-1} to 0.449 s^{-1} . Table 2 presents the comparisons of the experimental observations and predicted results with the integral model, followed by the relative errors. It can be seen that the trajectory and outline evolutions are almost overlapped in different cases before reaching maximum heights. However, both the maximum height and lock-up height become closer to the discharge height of the flow with the temperature gradient increasing, varying from −0.001 m to −0.083 m and −0.060 m to −0.145 m, respectively. It can be explained by Fig. 8 that in the ambient water with a large temperature gradient (shown with blue lines), the temperature of thermal jet flow can quickly decay to the background temperature after rising a short distance, otherwise, it will reach a higher layer in the water with a smaller temperature gradient (shown with red lines). In an extreme case where the temperature gradient is

close to 0, that is, the ambient fluid is thermally uniform (Case 1), the thermal flow will flow upwards to the water surface, as shown in the first row of Table 2. The relative error of the predicted lock-up height is below 7%, which is within the acceptable accuracy.

The thermal stratification layer at the bottom of the room has been used as an efficient strategy for energy saving, in the situation when the cool air is a part of air conditioning [15]. Furthermore, DV system is one HVAC system that is generally known to provide a good air quality by introducing 100% fresh supply close to the floor level and extracting contaminated air at a high level. However, the results in this study clarify that DV is not effective for indoor air quality when there is a large possibility of the pollutant trapping near people's breathing zone due to temperature gradients. It is also the main reason why DV system is not recommended in hospital environments in view of minimizing airborne transmission of respiratory pathogens [16]. In addition, thermal stratification also exists in ventilated built environments with under floor air distribution system [47] or nature ventilation driven by stack effect [48], in which cases it is significant to ensure that the lock-up layer of the exhaled airflow or pollutants are not trapped at the breathing zone. The findings can be used for a guidance of the early design and late performance for indoor ventilation system with respect to control the exhaled airborne pollutants. For example, increasing air change rate (ACH) can weaken the thermal stratification, as a result, the airborne pollutants will be locked at a higher height above the breathing zone, decreasing the exposure to the susceptible people.

Table 2
Comparisons of experimental and calculated results with different temperature gradients.

Case	Trajectories of thermal flow		Lock-up height (m)		
	Experiments	Predictions	Experiments	Predictions	Error
1			—	—	—
2			−0.060	−0.064	6.7%
3			−0.095	−0.099	4.2%
4			−0.135	−0.143	5.9%
5			−0.145	−0.149	2.8%

4.3. The effect of the exhalation velocity (scenario 2)

Non-isothermal jet flows with initial velocities of 2 m/s, 5 m/s and 10 m/s in Scenario 2 are designed to approximate the exhaled airflow produced during different respiratory modes. All parameters keep the same as Case 6 except the initial velocity. The evolutions of the reduced-scale thermal jet flow are shown in Table 3. In normal breathing with a small initial velocity (Case 6), an almost upward evolution of the thermal flow can be observed within a shorter distance, finally trapped at a higher lock-up height (−0.080 m). On the contrary, when the initial velocity increases to 10 m/s (Case 7), the thermal flow will travel a longer distance and upward motion becomes unobvious before reaching the maximum height, finally causing the lock-up height closer to the initial height. It can be seen in Table 1, for Scenario 2 the Fr number increases from 425 to 2126 with the increasing initial velocity. For the thermal flow the vertical momentum is induced by the buoyancy, which is fairly weak, thus the considerable horizontal momentum will dominate the dispersion of the exhaled flow. That means, after long distance in the horizontal direction the buoyant force can govern the flow. Since the temperature gradient is a constant in Scenario 2, it is suggested a larger Fr number could lead to lower stable lock-up height and maximum height of the buoyant flow. In addition, it can be found the jet width increases obviously with the initial velocity in both experimental and predicted results. It can be explained by the streamwise entrainment of ambient fluid into the turbulent jet flow, which is proportional to the centerline velocity of the jet flow [17]. In the observations of Case 7, it also shows that a stronger entrainment with a higher jet velocity will cause more turbulence in the jet flow, which in turn enhances the entrainment. Therefore, the exhalation airflow produced by intense respiratory activities, such as coughing and sneezing, could penetrate a long distance at the exhalation height. Some shielding measures for the respiratory source control are essential. Chen et al. [49] found that covering a cough with a tissue, a cupped hand, or an elbow can significantly reduce the horizontal velocity. In this case, the exhaled pollutants will be trapped at a higher layer above the breathing region, lowering the inhalation risk of susceptible people. In addition, placing a surgical mask on an infected patient can decrease the spread of aerosolized infections and offer a health-care worker more protection by reducing direct exposure [50].

4.4. The effect of the opening size in thermally stratified environment (scenario 3)

Scenario 3 are designed to explore the impact of the exhalation opening size on the exhaled airflow in stratified environments, with the results shown in Table 4. It is observed that the thermal flow with an opening of 0.025 m (Case 9) moves the longest distance of 0.35 m along the horizontal direction when travelling the same vertical distance as flows with opening sizes of 0.015 m (Case 8) and 0.020 m (Case 3). In addition, both the maximum height and lock-up height increase when

the opening size becomes larger, which can be explained by the Fr number here. In Scenario 3, the Fr number for is 1417, 1063 and 850 respectively, see Table 1. A smaller Fr number suggests a greater buoyant force here, thus the thermal flow can move more upward and consequently be locked at a higher layer. The buoyant force governs the upward motion after a horizontal distance of 0.25 m, 0.30 m and 0.35 m for each case respectively, and contributes to the trajectory be bent. The findings show that it should be paid more attention that when inhalation therapy nebulizers are used for the patients with respiratory diseases in hospital wards, the airflow carrying contagious pathogens discharged from a small orifice will finally trapped at a low height.

From all the case results in Tables 2–4, it is found that the predicted lock-up heights are slightly lower than the those in experiments. It is reasonable because the outlet of the L-like nozzle is not completely smooth, which weakens the initial momentum a bit, and finally causes a lower lock-up layer than the theoretical results. The deviation is also consistent with the findings of Scenario 2 in Table 3. Within the allowable range of error, it is considered that the integral model of an expiratory airflow can give an accurate prediction of the lock-up height and the upward outlines of a thermal jet flow in a stratified environment. Furthermore, it can be concluded from Scenarios 1–3 that the lock-up height is closely related to the initial state parameters of the thermal flow (i.e., the initial velocity and opening size) and the thermal stratification of the background fluid (i.e., temperature gradient). Fig. 9(a) summarizes the variation of the z_l with different N and Fr_0 in the experiments.

In the experiments, it is found that in the later spreading stage at the lock-up layer of the flow, the oscillations due to the blocking and feedback effect for internal density make the entrainment rate different from that of the steady upward flow. However, the effect is neglected in the theoretical model, causing the predicted oscillation is more obvious than the experimental observations. However, the results show that such error is relatively small for the lock-up height (z_l), a typical characteristic of the exhaled pollutants in indoor environments. The maximum height (z_m) and the thickness of the lock-up layer (h_l) in the later spreading stage (denoted in Fig. 8(b)) can be roughly estimated by z_l , as shown in Fig. 9.

Using regression techniques, z_l is found to vary with N and Fr_0 in the power law relation given in Fig. 9(a), and z_m and h_l tend to vary linearly with the z_l in Fig. 9(b). The experimental data can be used to give a quantitative validation of simplified theoretical models. Furthermore, the findings can provide implications for the ventilation performance in buildings and emergency responses to epidemic diseases to control or minimize the cross-infection risk.

4.5. Particle transport in both thermally uniform and stratified environments

The center vertical cross-section of the jet flow is illuminated by a laser to visualize the particle transport. The boundaries of the jet flow in

Table 3
Comparisons of experimental and calculated results with different initial velocities.


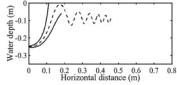

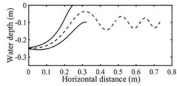
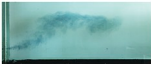
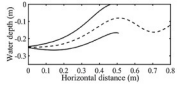

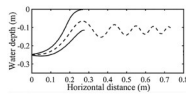

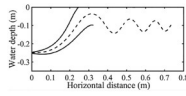
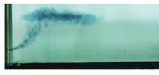
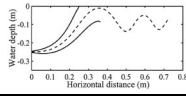
Case	Trajectories of thermal flow		Lock-up height (m)		
	Experiments	Predictions	Experiments	Predictions	Error
6			−0.080	−0.084	5.0%
3			−0.095	−0.099	4.2%
7			−0.110	−0.114	3.6%

Table 4
Comparisons of experimental and calculated results with different opening sizes.

Case	Trajectories of thermal flow		Lock-up height (m)		
	Experiments	Predictions	Experiments	Predictions	Error
8			-0.105	-0.120	14.2%
3			-0.095	-0.099	4.2%
9			-0.085	-0.089	4.7%

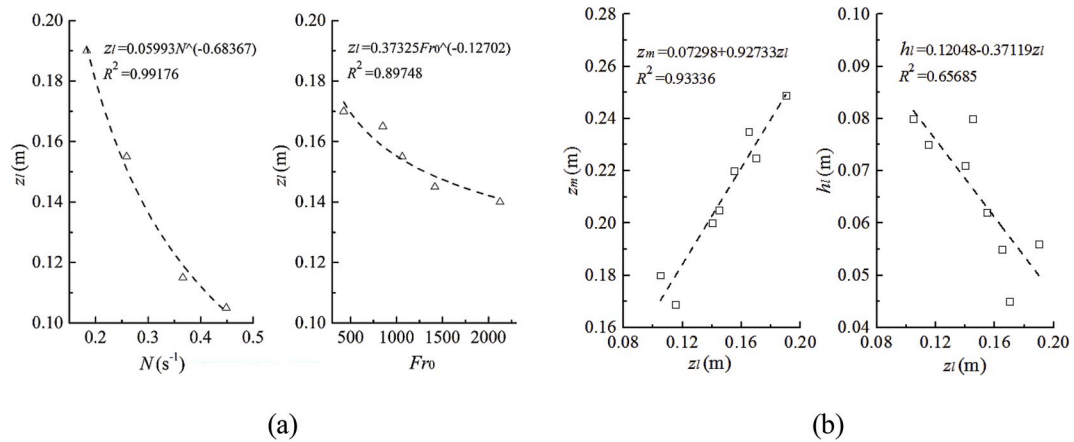


Fig. 9. Thermal flow rise in thermally stratified environments: (a) relationships between the lock-up height and N and Fr_0 ; (b) relationships between the rising heights.

thermally uniform and stratified water are consistent with those of Case 1 and Case 3, respectively. The pictures captured at 30s when the particle dispersion is steady are shown in dimensionless form (normalized by D) in Fig. 10, in which the red lines represent the predicted trajectory and outlines of the thermal flow.

It can be found that the particles with different sizes show obvious different trajectories. In thermally uniform environment, small particles (10–20 μm) can follow the thermal flow just like tracer gas. These

particles can almost fully fill in the whole region and finally concentrate on the water surface, with a vertical travel distance of about $62 D$. For medium particles (50–80 μm), most of them begin to escape form the upward flow and deposit downwards, with a maximum dispersion distance of about $50 D$. A small part can still disperse upwards with the thermal flow to about $38 D$, with a horizontal distance of about $57 D$. The largest particles (110–160 μm) can only travel about $25 D$ due to quick deposition. The particle distributions are consistent with those in the

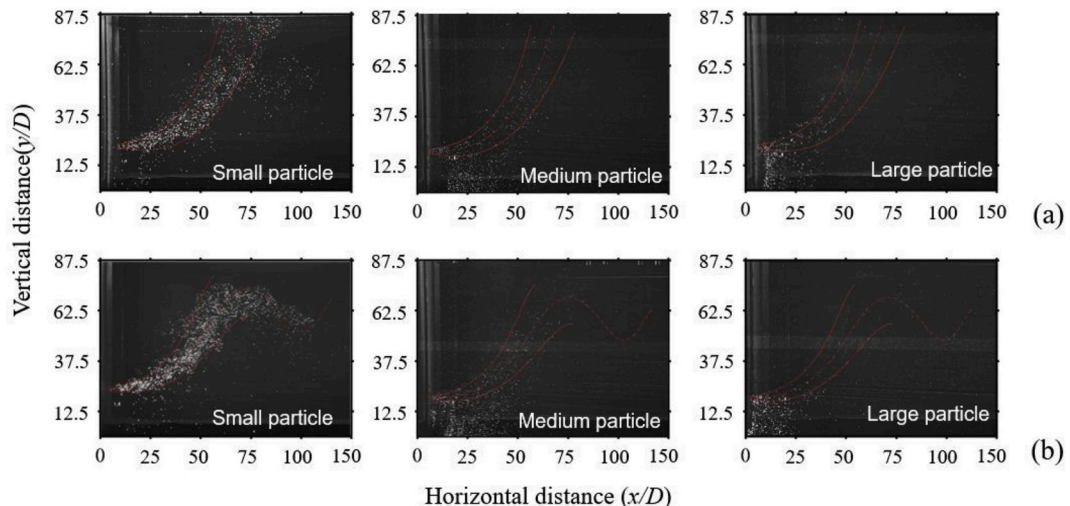


Fig. 10. Particle transport with a thermal jet flow: (a) In the thermally uniform environment; (b) In the thermally stratified environment.

theoretical work of Liu et al. [31]. It implies that in indoor environments, the exhaled particles of small sizes, such as fine droplets and droplet nuclei will be finally concentrated near the ceiling. In addition, the continuous increase of the jet width induced by the entrainment will promote the dilution of exhaled particles, and finally a homogeneous particle distribution could be made indoors. Therefore, the cross-infection risk is relatively low in this case.

Whereas in the thermally stratified environment, the results show that the lock-up phenomenon of the thermal flow causes a homogeneous distribution of small particles. The small particles firstly travelling upwards to about $62.5 D$ at a horizontal distance of about $70 D$. When the thermal flow dispersion cannot be continuously driven by buoyant force, the small particles will also be trapped with the flow, and travel a long horizontal distance of about $110 D$, much larger than that in the uniform environment. For medium particles, it can also be observed that some of them can travel with the flow, finally trapped at a height of about $60 D$, which is lower than the lock-up height of small particles. The rest escape from the thermal flow and deposit to a maximum distance of about $45 D$. The largest particles show a similar dispersion pattern with that in uniform environment, unaffected by the thermal stratification. It is suggested that in a ventilated room with a vertical temperature gradient (i.e., DV, under floor air distribution or natural ventilation), fine droplets or droplet nuclei exhaled by infectors will be transported farther away along the lock-up height, which could cause a long-range airborne infection risk between the infector and the susceptible people. It is important to predict whether the exhaled particles are trapped in the layer of the breathing zone of the susceptible to minimize the infection risk. Similar to the distribution in uniform environment, large droplets will deposit within a short distance, in which case droplet infection could happen to people at a close contact with the infector.

5. Limitations of the study

There are some limitations for current study. The exhalation flow is simplified to be steady in the present experiment, however, in a realistic exhalation activity, such as coughing, the exhaled flow is transient and generally characterized as a starting jet and an interrupt jet [43], which may produce slightly modified results, different from those in the present study. Therefore, the findings are mainly applicable to the early stage of design of an indoor environment. The pulsating breathing modes in realistic cases will be included and compared with the present steady jet flows in future experimental studies. In addition, some assumptions of the theoretical model for an expiratory airflow in a stratified environment, such as the tenets of self-similarity of the velocity and buoyancy and entrainment rate in the later spreading stage, are still needed to be validated or determined by more experimental investigations. Many studies demonstrate that the evaporation of the exhaled particles greatly affects the particle distribution, especially for small and medium particles [11,31]. The dispersion of large droplets and droplet nuclei can be respectively deduced by the large particles and small particles in this experimental study, while for medium droplets, the ignorance of the evaporation process may cause a deviation from the real situations. More detailed illustrations of the exhaled droplet transport and distribution in a stratified environment are also needed in future study.

6. Conclusions

A water tank experiment is designed to understand the evolution characteristics of the exhalation airflow and particles by human in both uniform and thermal stratified indoor environments. The impacts of thermal stratification intensity, exhalation velocity and opening size are considered here. Our experimental results show that the thermal jet can flow upwards freely in the uniform environment, and the temperature visualization also shows a gradual color decay along the flow trajectory. However, in the stratified environment, a temperature hump exists in

both experimental visualization and our previous simulations, illustrating the lock-up phenomenon indoors. Comparisons of the experimental and predicted results show that the integral model is effective to describe the upward outlines and lock-up trajectories of an expiratory airflow in thermally-stratified indoor environments. The lock-up height of the upward flow decreases in a power law relation with thermal stratification frequency N and Fr_0 . The discussion of the impacts of different factors on lock-up phenomenon can give some guidance to minimize the concentration exposure of the susceptible people, such as changing ACH in a ventilated environment and using shelters to weaken the expiratory intensity.

For the particle dispersion simulated in the water tank experiment, it is suggested that small particles, such as fine droplets and droplet nuclei can be concentrated at a certain height, and disperse along with the thermal flow over a long distance in a thermally-stratified indoor environment. It could induce a high long-range airborne infection risk between the infector and the susceptible people. Large particles such as large droplets, can quickly settle out of the flow region and deposit to the ground within a short distance, hardly being affected by indoor thermal stratification. Droplet infection could occur when the susceptible people are at a close contact with the infector. Findings in this study are expected to be useful for designing indoor environment and developing measures to minimize the airborne infection control especially in thermally stratified environment.

Declaration of interest statement

The authors declare no conflict of interest.

Acknowledgement

We sincerely appreciate the financial support by the National Natural Science Foundation of China (No. 51778128), the Scientific Research Foundation of Graduate School of Southeast University (No. YBJJ1806). The first author (F. Liu) would like to thank the financial support of China Scholarship Council (CSC) for academic visit at the University of Reading, where part of the research was conducted. We also would like to thank Haixin Wang and Chengcheng Shen for their technical assistance during the experiments.

References

- [1] F. Wu, S. Zhao, B. Yu, et al., A new coronavirus associated with human respiratory disease in China, *Nature* 579 (2020) 265–269, <https://doi.org/10.1038/s41586-020-2008-3>.
- [2] P. Zhou, X. Yang, X. Wang, et al., A pneumonia outbreak associated with a new coronavirus of probable bat origin, *Nature* 579 (2020) 270–273, <https://doi.org/10.1038/s41586-020-2012-7>.
- [3] Z.A. Memish, M. Cotten, B. Meyer, et al., Human infection with MERS coronavirus after exposure to infected camels, Saudi Arabia, *Emerg. Infect. Dis.* 20 (6) (2013) 1012–1015, 2014.
- [4] N.S. Zhong, B.J. Zheng, Y. Li, et al., Epidemiology and cause of severe acute respiratory syndrome (SARS) in Guangdong, People's Republic of China, in February, *Lancet* 362 (9393) (2003) 1353–1358.
- [5] W.F. Wells, *Airborne Contagion and Air Hygiene: an Ecological Study of Droplet Infection*, Harvard University Press, Cambridge, MA, USA, 1955.
- [6] P.V. Nielsen, Control of airborne infectious diseases in ventilated spaces, *J. R. Soc. Interface* 6 (2009) S747–S755.
- [7] Y. Li, G.M. Leung, J.W. Tang, et al., Role of ventilation in airborne transmission of infectious agents in the built environment—a multidisciplinary systematic review, *Indoor Air* 17 (2007) 2–18.
- [8] J. Wei, Y. Li, Airborne spread of infectious agents in the indoor environment, *Am. J. Infect. Contr.* 44 (2016) S102–S108.
- [9] Centers for Disease Control and Prevention (Cdc), Diseases & Conditions, U.S. Department of Health and Human Services, Atlanta, GA, 2019. <https://www.cdc.gov/DiseasesConditions>.
- [10] X. Xie, Y. Li, A. Chwang, et al., How far droplets can move in indoor environments—revisiting the Wells evaporation-falling curve, *Indoor Air* 17 (3) (2007) 211–225.
- [11] J. Wei, Y. Li, Enhanced spread of expiratory droplets by turbulence in a cough jet, *Build. Environ.* 93 (2015) 86–96.
- [12] L. Liu, Y. Li, P.V. Nielsen, et al., Short-range airborne transmission of expiratory droplets between two people, *Indoor Air* 27 (2016) 452–462.

- [13] P.V. Nielsen, I. Olmedo, M.R. de Adana, et al., Airborne cross-infection risk between two people standing in surroundings with a vertical temperature gradient, *HVAC R Res.* 18 (4) (2012) 552–561.
- [14] N. Gao, J. Niu, Numerical study of the lock-up phenomena of human exhaled droplets under a displacement ventilated room, *Building Simulation* 5 (1) (2012) 51–60.
- [15] Q. Zhou, H. Qian, H. Ren, et al., The lock-up phenomena of exhaled flow in a stable thermally-stratified indoor environment, *Build. Environ.* 116 (2017) 246–256.
- [16] H. Qian, Y. Li, P.V. Nielsen, et al., Dispersion of exhaled droplet nuclei in a two-bed hospital ward with three different ventilation systems, *Indoor Air* 16 (2006) 111–128.
- [17] F. Liu, C. Zhang, H. Qian, et al., Direct or indirect exposure of exhaled contaminants in stratified environments using an integral model of an expiratory jet, *Indoor Air* 29 (2019) 591–603.
- [18] H. Qian, P.V. Nielsen, Y. Li, et al., Airflow and contaminant distribution in hospital wards with a displacement ventilation system, in: *Built Environment and Public Health-Proceedings of BEPH2004*, China Environmental Science Press, Beijing, 2004, pp. 355–364.
- [19] X. Li, J. Niu, N. Gao, Spatial distribution of human respiratory droplet residuals and exposure risk for the co-occupant under different ventilation methods, *HVAC R Res.* 17 (2011) 432–445.
- [20] B. Zhao, Z. Zhang, X. Li, Numerical study of transport of droplets or particles generated by respiratory system indoors, *Build. Environ.* 40 (2005) 1032–1039.
- [21] P.V. Nielsen, J.J. Zajas, M. Litewnicki, et al., Breathing and cross-infection risk in the microenvironment around People, *Build. Eng.* 120 (1) (2014) 1–8.
- [22] E. Bjørn, P.V. Nielsen, Dispersal of exhaled air and personal exposure in displacement ventilated rooms, *Indoor Air* 12 (3) (2002) 147–164.
- [23] K.W. Mui, L.T. Wong, C.L. Wu, et al., Numerical modeling of exhaled droplet nuclei dispersion and mixing in indoor environments, *J. Hazard Mater.* 167 (1–3) (2009) 736–744.
- [24] H. Qian, Y. Li, P.V. Nielsen, et al., Dispersion of exhalation pollutants in a two-bed hospital ward with a downward ventilation system, *Build. Environ.* 43 (2008) 344–354.
- [25] A. Lai, S.L. Wong, Experimental investigation of exhaled aerosol transport under two ventilation systems, *Aerosol. Sci. Technol.* 44 (6) (2010) 444–452.
- [26] A. Lai, S.L. Wong, Expiratory aerosol transport in a scaled chamber under a variety of emission characteristics: an experimental study, *Aerosol. Sci. Technol.* 45 (8) (2011) 909–917.
- [27] Y. Ji, H. Qian, J. Ye, et al., The impact of ambient humidity on the evaporation and dispersion of exhaled breathing droplets: a numerical investigation, *J. Aerosol Sci.* 115 (2018) 164–172.
- [28] J.K. Gupta, C.-H. Lin, Q. Chen, Transport of expiratory droplets in an aircraft cabin, *Indoor Air* 21 (2011) 3–11.
- [29] J.K. Gupta, C.-H. Lin, Q. Chen, Characterizing exhaled airflow from breathing and talking, *Indoor Air* 20 (2010) 31–39.
- [30] J. Redrow, S. Mao, I. Celik, et al., Modeling the evaporation and dispersion of airborne sputum droplets expelled from a human cough, *Build. Environ.* 46 (2011) 2042–2051.
- [31] L. Liu, J. Wei, Y. Li, A. Ooi, Evaporation and dispersion of respiratory droplets from coughing, *Indoor Air* 27 (1) (2017) 179–190.
- [32] J.P. Duguid, The size and the duration of air-carriage of respiratory droplets and droplet-nuclei, *J. Hyg.* (1946) 471–479.
- [33] G.R. Hunt, P.F. Linden, The fluid mechanics of natural ventilation-displacement ventilation by buoyancy-driven flows assisted by wind, *Build. Environ.* 34 (1999) 707–720.
- [34] M.S. Davies Wykes, E. Chahour, P.F. Linden, The effect of an indoor-outdoor temperature difference on transient cross-ventilation, *Build. Environ.* 168 (2020) 106447.
- [35] Y. Fan, Y. Li, X. Wang, et al., A new convective velocity scale for studying diurnal urban heat island circulation, *J. Appl. Meteorol. Climatol.* 55 (2016) 2151–2164.
- [36] Y. Fan, Y. Li, S. Yin, Interaction of multiple urban heat island circulations under idealized settings, *Build. Environ.* 134 (2018) 10–20.
- [37] A.J. Ghajar, K. Bang, Experimental and analytical studies of different methods for producing stratified flows, *Energy* 18 (4) (1993) 323–334.
- [38] J.C.R. Hunt, W.H. Snyder, R.H.J. Lawson, Flow Structure and Turbulent Diffusion Around a Three-Dimensional Hill. Fluid Modeling Study on Effects of Stratification. Part 1: Flow Structure, 1978.
- [39] P. Frenzen, A Laboratory Investigation of the Lagrangian Autocorrelation Function in a Stratified Fluid, Argonne National Laboratory, 1963. ANL-6794.
- [40] Deardorff JW, Willis GE. Computer and laboratory modeling of the vertical diffusion of nonbuoyant particles in the mixed layer. *Adv. Geophys.*;18(18):187–200.
- [41] H.T. Liu, J.T. Lin, Laboratory Simulation of Plume Dispersion in Stably Stratified Flows over Complex Terrain: Phase 2, Flow Research, Inc., Kent, Washington, 1975. Report No. 57.
- [42] J. Lu, S.P. Arya, W.H. Snyder, et al., A laboratory study of the urban heat island in a calm and stably stratified environment. Part II: velocity field, *J. Appl. Meteorol.* 36 (1997) 1392–1402.
- [43] J. Wei, Y. Li, Human cough as a two-stage jet and its role in particle transport, *PLoS One* 12 (1) (2017), e0169235.
- [44] A.A. Townsend, The Structure of Turbulent Shear Flow, Cambridge Univ. Press, Cambridge, England, 1956, p. 315.
- [45] P. Hoppe, Temperatures of expired air under varying climatic conditions, *Int. J. Biometeorol.* 25 (2) (1981) 127–132.
- [46] A. De Visscher, Air Dispersion Modeling: Foundations and Applications, Wiley, New York, 2013.
- [47] X. Wang, C. Huang, W. Cao, et al., Experimental study on indoor thermal stratification in large space by under floor air distribution system (UFAD) in summer, *Engineering* 3 (2011) 384–388.
- [48] M.A. Menchaca-Brandan, Study of Airflow and Thermal Stratification in Naturally Ventilated Rooms, Massachusetts Institute of Technology, 2012.
- [49] C. Chen, C.H. Lin, Z. Jiang, et al., Simplified models for exhaled airflow from a cough with the mouth covered, *Indoor Air* 24 (2014) 580–591.
- [50] M.M. Mansour, G.C. Smaldone, Respiratory source control versus receiver protection: impact of facemask fit, *J. Aerosol Med. Pulm. Drug Deliv.* 26 (2013) 131–137.